High quantum efficiency InGaN/GaN solar cells with 2.95 eV band gap

Carl J. Neufeld,[1,a)] Nikholas G. Toledo,[1] Samantha C. Cruz,[2] Michael Iza,[2] Steven P. DenBaars,[2] and Umesh K. Mishra[1]
[1]*Department of Electrical and Computer Engineering, University of California at Santa Barbara, Santa Barbara, California 93106, USA*
[2]*Materials Department, University of California at Santa Barbara, Santa Barbara, California 93106, USA*

(Received 19 August 2008; accepted 3 September 2008; published online 8 October 2008)

We report on III-nitride photovoltaic cells with external quantum efficiency as high as 63%. $In_xGa_{1-x}N/GaN$ *p-i-n* double heterojunction solar cells are grown by metal-organic chemical vapor deposition on (0001) sapphire substrates with $x_{In}=12\%$. A reciprocal space map of the epitaxial structure showed that the InGaN was coherently strained to the GaN buffer. The solar cells have a fill factor of 75%, short circuit current density of $4.2\ mA/cm^2$, and open circuit voltage of 1.81 V under concentrated AM0 illumination. It was observed that the external quantum efficiency can be improved by optimizing the top contact grid. © *2008 American Institute of Physics.*
[DOI: 10.1063/1.2988894]

The (In,Al,Ga)N material system has proven itself in both electronic and optoelectronic applications. High electron mobility transistors are gaining popularity in high-power and high-speed electronics, while light emitting diodes and laser diodes based on this material system are revolutionizing the lighting, display, and data storage industries.[1,2]

Recently, III-nitrides (III-Ns) have begun to gain attention for use in photovoltaic (PV) devices.[3,4] InGaN has many material properties that make it an excellent candidate for high efficiency PV devices. InGaN alloys have been shown to have superior high energy radiation resistance for space based PV applications.[5] The band gap of InN was recently discovered to be 0.7 eV as opposed to the previously believed 1.3 eV.[6–9] The importance of this discovery is that the band gap of the InGaN material system spans nearly the entire solar spectrum (0.7–3.4 eV), thus enabling design of multijunction solar cell structures with near ideal band gaps for maximum efficiency. Even more interesting is that the band gap is direct for the entire material system. This is in contrast to the AlGaAs and AlGaP systems whose band gap is indirect for higher band gap alloys.[10,11]

The III-N alloys also tend to exhibit very strong absorption of approximately $10^5\ cm^{-1}$ at the band edge,[12,13] allowing a large fraction of the incident light to be absorbed in a few hundred nanometers of material. This is in contrast to the tens or hundreds of microns of material as is necessary in traditional Si solar cells.[14,15]

The III-N material system does however present challenges to the device designer. The lack of cheaply available defect-free native substrates presents a significant challenge. The III-N crystals grown on sapphire contain relatively high densities of threading dislocations, which have been shown to negatively impact GaN *p-n* junction device performance by increasing leakage current.[16] Another difficulty is the large lattice mismatch between InN and GaN, making it difficult to grow good quality material with high In content due to *V*-pit formation[17] and InN segregation.[13]

In this letter we report on the results of InGaN/GaN double heterojunction *p-i-n* solar cell devices. All devices were grown by metal-organic chemical vapor deposition (MOCVD) on (0001) sapphire substrates. The typical device structure is shown in Fig. 1.

Strain relaxation can result in defect formation that can increase nonradiative recombination[18] and in turn degrade solar cell performance. In order to obtain the highest quality InGaN possible, we wanted to ensure that the InGaN layer was coherently strained to the GaN layer below it.

An x-ray diffraction (XRD) reciprocal space map taken around the asymmetric (105) reflection for a typical solar cell structure is shown in Fig. 2. It can be observed that for this sample with an InGaN thickness of 200 nm, the layer is coherently strained to the GaN buffer. The indium content was determined to be 12% from a symmetric (004) ω-2θ scan (see Fig. 3), which corresponds to a band gap of 2.95 eV using a band gap bowing parameter of 1.43 eV.[19] This value is also confirmed by measured peak photoluminescence emission at 417 nm.

The material was processed into $0.5\times0.5\ mm^2$ mesas by contact lithography and inductively coupled plasma etch-

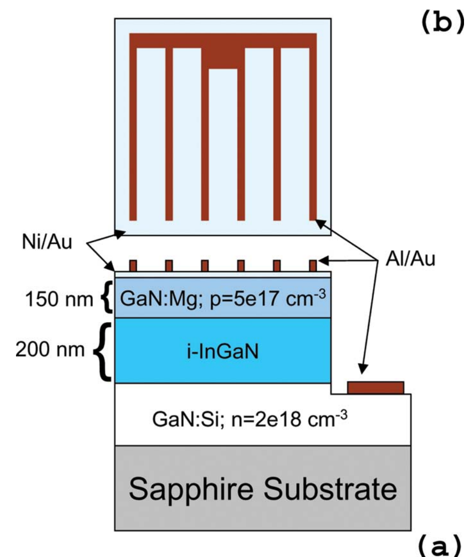

FIG. 1. (Color online) InGaN/GaN solar cell device structure (a) and contact grid layout (b).

[a)]Electronic mail: cjn@umail.ucsb.edu.

 © 2008 American Institute of Physics

Downloaded 29 Oct 2008 to 129.8.164.170. Redistribution subject to AIP license or copyright; see http://apl.aip.org/apl/copyright.jsp

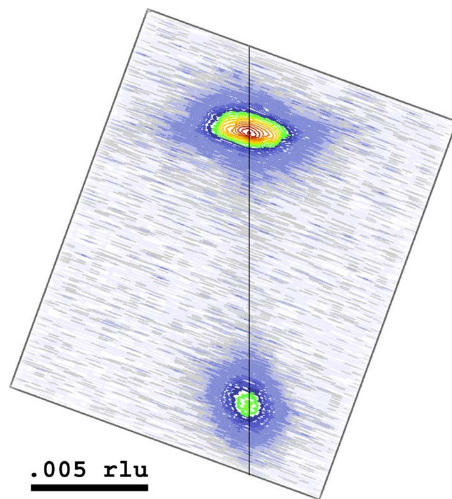

FIG. 2. (Color online) Reciprocal space map around the asymmetric (105) reflection of InGaN/GaN solar cell structure showing InGaN coherently strained to GaN.

ing with Cl_2 gas. Semitransparent Ohmic contacts to *p*-GaN were formed by electron beam evaporation of Ni/Au (5 /5 nm) on the entire mesa and subsequent rapid thermal annealing at 500 °C in O_2 for 5 min. An Al/Au grid was deposited on top of the Ni/Au with 5 μm wide grid lines and center-to-center grid spacing ranging from 25 to 166 μm. The area shaded by the grid lines ranges from 20.5% to 5.6% of the mesa area. Contacts to *n*-GaN were formed by evaporation of Al/Au and subsequent lift-off. No antireflection coating or surface passivation was used.

The current-voltage characteristics were measured with a Keithley 2632 source meter. The devices were illuminated with an Oriel solar simulator with a Xe lamp and AM0 filter. Monochromatic illumination for quantum efficiency measurements was supplied by coupling the Xe lamp to an Oriel 260 monochromator with a spectral linewidth of <5 nm full width at half maximum as measured with an Ocean Optics USB2000 spectrometer.

Measured solar cell parameters for typical devices with 25 and 166 μm grid spacing are summarized in Table I. The devices with 166 μm grid spacing demonstrated high peak external quantum efficiency (η_e) of 63% at 392 nm and a flat

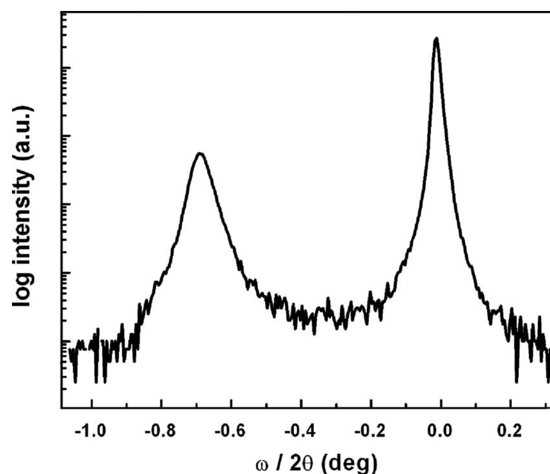

FIG. 3. (004) reflection ω-2θ XRD scan of the $In_xGa_{1-x}N$/GaN solar cell structure with x_{In}=0.12.

TABLE I. Measured solar cell parameters.

Contact spacing	V_{OC} (V)	FF (%)	J_{sc} (mA/cm^2)	P_{MAX} (mW/cm^2)	Peak EQE (%)
25 μm	1.75	75.1	3.5	4.6	51
166 μm	1.81	75.3	4.2	5.7	63

($\pm$3%) quantum efficiency response from 370 to 410 nm as shown in Fig. 4. The external quantum efficiency of these devices is limited by several factors: reflection at the surface, absorption in the semitransparent Ni/Au current spreading layer, and incomplete absorption in the InGaN layer. An estimated peak internal quantum efficiency η_i of 94% can be calculated using the following equation from Ref. 20: $\eta_i = \eta_e / \{(1-R)(1-S)[1\text{-exp}(-\alpha d)]\}$, where R is the reflectivity at the top surface (~0.18 for air-GaN interface),[20,21] S is the fraction of the mesa area shaded by the contact grid (0.056 for the 166 μm grid spacing), α is the absorption coefficient of the InGaN (10^5 cm^{-1}),[12,13] and d is the InGaN thickness. This estimate does not take into account the absorption in the Ni/Au contact layer; therefore, the actual internal quantum efficiency may be higher. Comprehensive studies of the absorption and reflectivity values for these structures are underway and will be reported in detail shortly. The low quantum efficiency performance below 360 nm is due to absorption in the *p*-GaN layer and can be improved by optimizing the thickness of this layer or using a window layer with a large band gap such as AlGaN.

Current and power density versus voltage characteristics for devices with 166 and 25 μm grid spacing under concentrated AM0 illumination are shown in Fig. 5. Short circuit current density for the devices with 166 μm grid spacing was 20% higher than that of the 25 μm device, which corresponds very closely to the 19% increase in unshaded device area. The devices with a 25 μm grid demonstrated a very high fill factor of 75.1% indicating excellent solar cell performance. It should be noted that the device with 166 μm grid spacing did not suffer any substantial degradation in the *J*-*V* performance. In fact, the 166 μm devices had

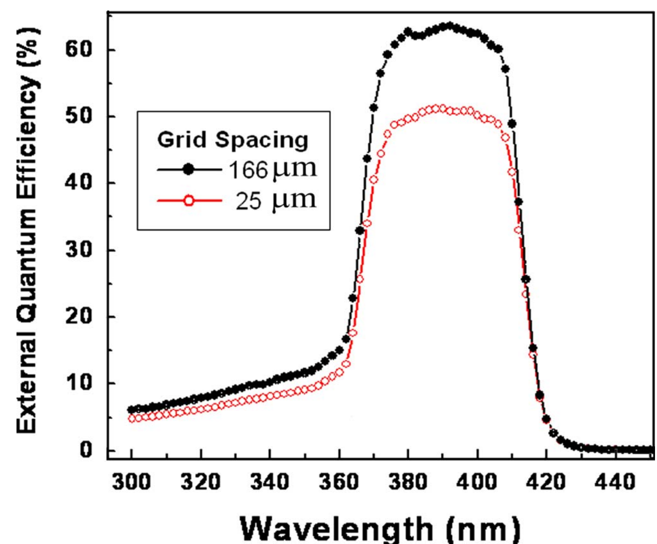

FIG. 4. (Color online) External quantum efficiency vs wavelength for InGaN/GaN pin solar cells with top contact grid spacing of 166 μm (solid circles) and 25 μm (open circles).

Downloaded 29 Oct 2008 to 129.8.164.170. Redistribution subject to AIP license or copyright; see http://apl.aip.org/apl/copyright.jsp

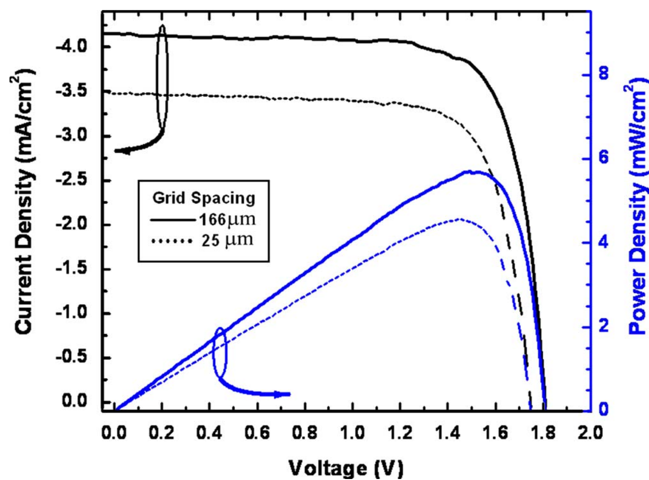

FIG. 5. (Color online) Typical *J-V* and power density vs voltage characteristic for InGaN/GaN pin solar cell under concentrated AM0 illumination for 166 μm (solid line) and 25 μm (dashed line) contact grid spacing.

a fill factor of 75.3%, nearly identical to the 25 μm devices, and enhanced open circuit voltage from 1.75 to 1.81 V. The identical fill factor and increased open circuit voltage coupled with the enhanced short circuit current density resulted in a 24% increase in maximum power density for the device with the optimized 166 μm contact grid.

To conclude, double heterojunction solar cells processed from coherently strained high-quality $In_{0.12}Ga_{0.88}N$ films grown by MOCVD on sapphire resulted in devices with fill factors greater than 75%. By optimizing the *p*-contact grid spacing, peak external quantum efficiency greater than 60% was achieved. Furthermore, the quantum efficiency spectrum showed a flat spectral response from 370 to 410 nm. The efficiency of the III-N solar cells can be further improved by optimizing the *p*-GaN contact such as optimizing the Ni and Au thicknesses and exploring alternate contact schemes such as indium tin oxide and zinc oxide. The short wavelength response could be enhanced by using *p*-AlGaN as a window layer instead of *p*-GaN. This should have the added benefit of potentially reducing the recombination of electrons at the surface. Additionally, an antireflection coating on the top surface should also increase the performance of these devices.

This work is funded by the Solid-State Lighting and Energy Center (SSLEC) at UC Santa Barbara. This work was partially supported by the Department of Defense (DoD) through the National Defense Science and Engineering Graduate (NDSEG) Fellowship Program and MRSEC Program of the National Science Foundation under Award No. DMR05-20415.

[1] S. Nakamura and G. Fasol, *The Blue Laser Diode* (Springer, Berlin, 2000).
[2] S. J. Pearton and F. Ren, Adv. Mater. (Weinheim, Ger.) **12**, 1571 (2000).
[3] X. Zhang, X. Wang, H. Xiao, C. Yang, J. Ran, C. Wang, Q. Hou, and J. L. Li, J. Phys. D **40**, 7335 (2007).
[4] O. Jani, I. Ferguson, C. Honsberg, and S. Kurtz, Appl. Phys. Lett. **91**, 132117 (2007).
[5] J. Wu, W. Walukiewicz, K. M. Yu, W. Shan, J. W. Ager III, E. E. Haller, H. Lu, W. J. Schaff, W. K. Metzger, and S. Kurtz, J. Appl. Phys. **94**, 6477 (2003).
[6] V. Davydov, A. Klochikhin, R. Seisyan, V. Emtsev, S. Ivanov, F. Bechstedt, J. Furthmüller, H. Harima, A. Mudryi, J. Aderhold, O. Semchinova, and J. Graul, Phys. Status Solidi B **229**, r1 (2002).
[7] J. Wu, W. Walukiewicz, K. M. Yu, J. W. Ager III, E. E. Haller, H. Lu, W. J. Schaff, Y. Saito, and Y. Nanishi, Appl. Phys. Lett. **80**, 3967 (2002).
[8] T. Matsuoka, H. Okamoto, M. Nakao, H. Harima, and E. Kurimoto, Appl. Phys. Lett. **81**, 1246 (2002).
[9] Y. Saito, H. Harima, E. Kurimoto, T. Yamaguchi, N. Teraguchi, A. Suzuki, T. Araki, and Y. Nanishi, Phys. Status Solidi B **234**, 796 (2002).
[10] A. J. Ekpunobi and A. O. E. Animalu, Superlattices Microstruct. **31**, 247 (2002).
[11] D. E. Aspnes and A. A. Studna, Phys. Rev. B **27**, 985 (1983).
[12] J. F. Muth, J. H. Lee, I. K. Shmagin, R. M. Kolbas, J. Casey, B. P. Keller, U. K. Mishra, and S. P. DenBaars, Appl. Phys. Lett. **71**, 2572 (1997).
[13] R. Singh, D. Doppalapudi, T. D. Moustakas, and L. T. Romano, Appl. Phys. Lett. **70**, 1089 (1997).
[14] L. Zeng, Y. Yi, C. Hong, J. Liu, N. Feng, X. Duan, L. C. Kimerling, and B. A. Alamariu, Appl. Phys. Lett. **89**, 111111 (2006).
[15] D. Redfield, Appl. Phys. Lett. **25**, 647 (1974).
[16] P. Kozodoy, J. P. Ibbetson, H. Marchand, P. T. Fini, S. Keller, J. S. Speck, S. P. DenBaars, and U. K. Mishra, Appl. Phys. Lett. **73**, 975 (1998).
[17] I. Kim, H. Park, Y. Park, and T. Kim, Appl. Phys. Lett. **73**, 1634 (1998).
[18] Y. H. Kim, C. S. Kim, S. K. Noh, J. Y. Leem, K. Y. Lim, B. S. O, and J. P. Song, in *Materials and Devices for Optoelectronics MRS Proceedings Volume 722*, edited by R. B. Wehrspohn, R. März, S. Noda, and C. Soukoulis (Materials Research Society, Pittsburgh, 2002), p. 193.
[19] J. Wu, W. Walukiewicz, K. M. Yu, J. W. Ager III, E. E. Haller, H. Lu, and W. J. Schaff, Appl. Phys. Lett. **80**, 4741 (2002).
[20] E. A. Berkman, N. A. El-Masry, A. Emara, and S. M. Bedair, Appl. Phys. Lett. **92**, 101118 (2008).
[21] M. J. Bergmann, U. Ozgur, J. Casey, H. O. Everitt, and J. F. Muth, Appl. Phys. Lett. **75**, 67 (1999).

Downloaded 29 Oct 2008 to 129.8.164.170. Redistribution subject to AIP license or copyright; see http://apl.aip.org/apl/copyright.jsp